Published in final edited form as:
J Nucl Med. 2018 August ; 59(8): 1296–1301. doi:10.2967/jnumed.117.206979.

In vivo characterization of four ^{68}Ga-labelled multimeric RGD peptides to image $\alpha_v\beta_3$ integrin expression in two human tumour xenograft mouse models

Daphne Lobeek[1], **Gerben M. Franssen**[1], **Michelle T. Ma**[2], **Hans-Jürgen Wester**[3], **Clemens Decristoforo**[4], **Wim J. G. Oyen**[1,5], **Otto C. Boerman**[1], **Samantha Y. A. Terry**[#2], and **Mark Rijpkema**[#1]

[1]Department of Radiology and Nuclear Medicine, Radboud University Medical Center Nijmegen, Nijmegen, The Netherlands [2]Department of Imaging Chemistry and Biology, King's College London, London, United Kingdom [3]Pharmazeutische Radiochemie, Technische Universität München, Garching, Germany [4]Clinical Department of Nuclear Medicine, Medical University Innsbruck, Innsbruck, Austria [5]Department of Nuclear Medicine, Institute of Cancer Research, Royal Marsden NHS Trust, London, United Kingdom

[#] These authors contributed equally to this work.

Abstract

Rationale—$\alpha_v\beta_3$ integrins play an important role in angiogenesis and cell migration of tumours. They are highly expressed on activated endothelial cells of newly formed blood vessels. Here, we compare the targeting characteristics of four ^{68}Ga-labelled multimeric cyclic RGD-based tracers in an $\alpha_v\beta_3$ integrin-expressing tumour model and in a tumour model where $\alpha_v\beta_3$ integrin is expressed solely on the neovasculature.

Methods—Female BALB/c nude mice were subcutaneously injected with SK-RC-52 ($\alpha_v\beta_3$ integrin-positive) or FaDu ($\alpha_v\beta_3$ integrin-negative) tumour cells. ^{68}Ga-labelled DOTA-E-[c(RGDfK)]$_2$ TRAP-(RGD)$_3$, FSC-(RGD)$_3$, or THP-(RGD)$_3$ were intravenously administered to the mice (0.5 nmol per mouse, 10-15 MBq), followed by microPET/CT imaging and *ex vivo* biodistribution studies one hour post injection. Nonspecific uptake of the tracers in both models was determined by co-injecting an excess of unlabelled DOTA-E-[c(RGDfK)]$_2$ (50 nmol) along with the radiolabelled tracers.

Results—Imaging and biodistribution data showed specific uptake in the tumours for each tracer in both tumour models. Tumour uptake of ^{68}Ga-FSC-(RGD)$_3$ was significantly higher than that of ^{68}Ga-DOTA-E-[c(RGDfK)]$_2$, ^{68}Ga-TRAP-(RGD)$_3$, and ^{68}Ga-THP-(RGD)$_3$, in the SK-RC-52 model, but not in the FaDu model, where ^{68}Ga-FSC-(RGD)$_3$ showed significantly higher tumour uptake than ^{68}Ga-TRAP-(RGD)$_3$. Most importantly, differences were also observed in normal tissues and in tumour-to-blood ratios.

Correspondence to: D. Lobeek (daphne.lobeek@radboudumc.nl) Department of Radiology and Nuclear Medicine, Radboud University Medical Centre, P.O. Box 9101, 6500 HB, Nijmegen, Netherlands, telephone number: +31 (0) 24 361 45 10, fax number: +31 (0) 24 361 89 42.

Europe PMC Funders Author Manuscripts

Conclusion—All tracers showed sufficient targeting of $\alpha_v\beta_3$ integrin expression to allow tumour detection. While the highest tumour uptake was found for ^{68}Ga-FSC-(RGD)$_3$ and ^{68}Ga-THP-(RGD)$_3$ in the SK-RC-52 and FaDu model, respectively, tumour-to-blood ratio and uptake in normal tissues should also be considered in selecting the most optimal tracer for specific diagnostic or therapeutic applications with radiolabelled RGD peptides.

Introduction

Molecular imaging of $\alpha_v\beta_3$ integrin expression with SPECT (Single-Photon Emission Computed Tomography) or PET (Positron Emission Tomography) is a promising technique that allows for imaging of tumour angiogenesis. $\alpha_v\beta_3$ integrins are transmembrane proteins, recognizing the arginine-glycine-aspartate (RGD) sequence of extracellular matrix proteins. $\alpha_v\beta_3$ integrins are expressed on the tumour cell membrane of several solid tumours, thereby modulating tumour growth and metastases [1]. During the process of angiogenesis, activated $\alpha_v\beta_3$ integrins are expressed on endothelial cells of newly formed vessels, inducing gene-expression and cytoskeleton changes and regulating cell growth and survival of tumour cells [2]. $\alpha_v\beta_3$ integrins are studied as targets for tumour-targeted therapies [3], RGD-drug conjugates [4], and as a target for molecular imaging agents to further characterize tumours and predict and/or assess response of anti-angiogenic cancer therapies. [5].

A series of RGD analogues for *in vivo* imaging of $\alpha_v\beta_3$ integrins have been developed with different approaches to obtain ligands with a high *in vivo* stability, high affinity for $\alpha_v\beta_3$ integrins, and optimal pharmacokinetics [6]. It has been shown that cyclization of linear RGD peptides and multimerization improved the binding affinity of RGD ligands for $\alpha_v\beta_3$ integrins [7–10]. For wider adoption of PET and SPECT imaging of $\alpha_v\beta_3$ integrin expression in the clinic, radiolabelled ligands require straightforward, robust, and efficient labelling protocols. The most recently developed ligands can be radiolabelled very efficiently (>90%) and rapidly (<15 minutes) with gallium-68 (^{68}Ga), making them suited ligands for clinical applications. Because of the excellent physical characteristics of ^{68}Ga (short half-life (68 minutes), high positron yield (89%)), and the availability of GMP-compliant ^{68}Ge/^{68}Ga generators, ^{68}Ga-labelled RGD peptides can now be considered as tracers for PET imaging of angiogenesis.

Major efforts have been made in developing stable ^{68}Ga-labelled RGD peptides and several different monomeric ^{68}Ga-binding bifunctional chelators were considered [11, 12], of which ^{68}Ga-NOTA-RGD was already studied in lung cancer- and lymphoma patients [11]. However, dimeric, trimeric, and tetrameric RGD analogues have shown higher specific accumulation in $\alpha_v\beta_3$ integrin expressing tumours compared to their monomeric counterparts [7–10]. Four recently developed multimeric ^{68}Ga-labelled RGD peptides, with good *in vivo* imaging characteristics, are ^{68}Ga-DOTA-E-[c(RGDfK)]$_2$ [7, 8], ^{68}Ga-TRAP-(RGD)$_3$ [13, 14], ^{68}Ga-FSC-(RGD)$_3$ [15, 16], and ^{68}Ga-THP-(RGD)$_3$ [17]. These four multimeric ^{68}Ga-labelled $\alpha_v\beta_3$ integrin-targeted tracers have been used in preclinical studies to investigate the *in vitro*, *in vivo*, and *ex vivo* targeting characteristics and their potential for clinical application [8, 13–17]. However, all four RGD peptides have been tested in separate experiments using different murine tumour models with high levels of $\alpha_v\beta_3$ integrin expression. To directly compare the imaging characteristics of these ^{68}Ga-labelled RGD

Europe PMC Funders Author Manuscripts

Europe PMC Funders Author Manuscripts

peptides, here we assessed the *in vivo* and *ex vivo* behaviour in both $\alpha_v\beta_3$ integrin-positive (SK-RC-52) and $\alpha_v\beta_3$ integrin-negative (FaDu, $\alpha_v\beta_3$ integrin expression only on neovasculature) human xenograft tumour models in the same experimental set-up and under standardized conditions.

Materials and Methods

Synthesis and Radiolabelling RGD Peptides

The RGD peptides DOTA-E-[c(RGDfK)]$_2$ (Molecular weight 1704.8 g/mol), TRAP-(RGD)$_3$ (Molecular weight 3145.0 g/mol), FSC-(RGD)$_3$ (Molecular weight 2782.3 g/mol), and THP-(RGD)$_3$ (Molecular weight 3720.6 g/mol) were synthesized as described in previous studies [7, 8, 13–17]. The structures of the four RGD peptides are shown in figure 1. The four RGD peptides were labelled with ^{68}Ga eluted from a GG100 TiO_2-based ^{68}Ge/^{68}Ga generator (Eckert & Ziegler, Berlin, Germany) eluted with 0.1 M HCl. Three fractions of 1 mL were collected and the second fraction (fraction with the highest activity) was used for labelling the peptides.

^{68}Ga-labelled DOTA-E-[c(RGDfK)]$_2$ (6 μg) and TRAP-(RGD)$_3$ (11 μg) were prepared by mixing the RGD peptide (1 μg/μL), ^{68}Ga (700 μL, 142-168 MBq), and 1.0 M HEPES buffer (88 μL) for 20 minutes (DOTA-E-[c(RGDfK)]$_2$) or 5 minutes (TRAP-(RGD)$_3$) at 95°C. ^{68}Ga-labelled FSC-(RGD)$_3$ (10 μg) and THP-(RGD)$_3$ (13 μg) were prepared by mixing the RGD peptide (1 μg/μL), ^{68}Ga-eluate (700 μL, 105-196 MBq), and 150 μL 0.5 M NaOAc, in an Eppendorf LoBind™ tube for 15 minutes at room temperature.

All tracers were further diluted to 15 MBq/0.3 ml in 0.1 M phosphate buffered saline (PBS) with 0.5% Bovine Serum Albumin (BSA) at pH (pH 7.4) for *in vivo* studies.

Quality Control

Instant thin-layer chromatography (ITLC) analysis of all four ^{68}Ga-labelled RGD peptides was performed with silica gel chromatography strips (Agilent Technologies), using 0.1M NH_4OAc/0.1M EDTA (1:1 v/v) as mobile phase. The strips were analyzed using a Fujifilm BAS-1800II Scanner (Fuji Photo Film Co., Tokyo, Japan) and Aida Software (version 4.21, Raytest GmbH, Straubenhardt, Germany).

The radiochemical purities were also determined by reverse-phase high-performance liquid chromatography (RP-HPLC) on the Agilent 1100 system (Agilent Technologies, Palo Alto, CA, USA) using a C18 column (RX-C18, 4.6×250 mm, Zorbax) eluted with a gradient mobile phase [0–5 min 97% buffer A, 5–15 min 97% buffer A to 0% buffer A (buffer A = 0.1% trifluoroacetic acid (TFA) in H_2O, buffer B = B=0.1% TFA in acetonitrile)] at 1 mL/min. The radioactivity of the eluate was monitored using an in-line NaI radiodetector. Elution profiles were analyzed using Gina Star software (version 5.9, Raytest GmbH, Straubenhardt, Germany).

Solid-Phase $\alpha_v\beta_3$ Integrin Binding Assay

The IC_{50} of DOTA-E-[c(RGDfK)]$_2$, TRAP-(RGD)$_3$, FSC-(RGD)$_3$, and THP-(RGD)$_3$ for binding $\alpha_v\beta_3$ integrin was determined using a solid-phase competitive binding assay, with

^{111}In-labelled DOTA-E-[c(RGDfK)]$_2$ (6 MBq/μg) as the read-out tracer. The binding assays were carried out as described previously [8]. ^{111}In-labelled DOTA-E-[c(RGDfK)]$_2$ was prepared by adding 29.9 μL (16 MBq) $^{111}InCl_3$ solution to 1 μL peptide dissolved in 60 μL 0.5M MES buffer (2-(N-morpholino)ethanesulfonic acid), pH 5.5, and was further purified on an Oasis® HLB (1 cm^3, 30 mg) cartridge (Waters, Milford, MA, USA). Radiochemical purity was determined by ITLC.

Two 96-well vinyl microtiter plates (Corning B.V., Schiphol-Rijk, The Netherlands) were coated with a solution of purified human $\alpha_v\beta_3$ integrin (150 ng/mL, 100 μL/well) (Chemicon International, Temecula, CA, USA) in coating buffer (25 mM Tris-HCl, pH 7.4, 150 mM NaCl, 1 mM $CaCl_2$, 0.5 mM $MgCl_2$ and 1 mM $MnCl_2$). Non-specific binding was assessed by blocking with 1% BSA in coating buffer (200 μL/well). The appropriate peptide dilution (3 μM to 5x10^{-5} μM, 50 μL/well) and ^{111}In-DOTA-E-[c(RGDfK)]$_2$ (50 μL/well) was added. After incubation, wells were washed and cut out of the plates. The amount of radioactivity in each well was counted in the gamma counter (PerkinElmer Inc, Waltham, MA, USA), along with 1% standards. For each tracer, triplicate measurements were performed.

Cell Lines and Animal Studies

The *in vivo* behaviour of ^{68}Ga-DOTA-E-[c(RGDfK)]$_2$, ^{68}Ga-TRAP-(RGD)$_3$, ^{68}Ga-FSC-(RGD)$_3$, or ^{68}Ga-THP-(RGD)$_3$ was determined in two different tumour models in athymic mice. First, mice were used with subcutaneous SK-RC-52 human renal cell carcinoma xenografts (tumour cells expressing $\alpha_v\beta_3$ integrins on both tumour cell membrane and neovasculature; $\alpha_v\beta_3$ integrin-positive tumours). Second, to study the RGD uptake in tumour neovasculature only, mice were used with subcutaneous FaDu human squamous cell carcinomas ($\alpha_v\beta_3$ integrin expressed solely on neovasculature; $\alpha_v\beta_3$ integrin-negative tumours [18]). Both tumour cell lines were obtained from the American Type Culture Collection (Molsheim Cedex, France) and cultured in Roswell Park Memorial Institute (RPMI) 1640 medium (Gibco, BRL Life Sciences Technologies, The Netherlands), supplemented with 1% glutamine (Gibco) and 10% fetal calf serum (Sigma-Aldrich Chemie BV, Zwijndrecht, The Netherlands) (RPMI+) at 37°C in a humidified atmosphere with 5% CO_2. Before subcutaneous inoculation, tumour cells were washed in PBS, harvested with 0.25% trypsin (5 minutes at 37°C in a humidified atmosphere with 5% CO_2), counted, spun down (5 minutes at 1000x*g*) and resuspended to the appropriate concentration with RPMI+. Mice were injected subcutaneously in the left flank with SK-RC-52 cells (2x10^6 cells in 0.2 mL RPMI+ per mouse) or FaDu cells (4.5x10^6 cells in 0.2 mL RPMI+ per mouse). Tumours were allowed to grow until they reached a volume of approximately 200 mm^3 as determined by caliper measurements in three dimensions.

The animal studies were approved by The Animal Welfare Body of the Radboud University Medical Centre Nijmegen and were performed in accordance with the Dutch legislation (Dutch Act on Animal Experimentation). Female athymic BALB/c nude mice (6- to 8-week old BALB/c nu/nu/Foxn1nu, Janvier, n=64) acclimatized for seven days after transportation to the animal facility. The mice were housed in filter-topped cages (3 or 5 mice/cage) in a specific pathogen-free unit under standard laboratory conditions (day-night rhythm, 12-12 h;

room temperature, 20-24 °C; relative humidity, 50-60 %) and had free access to water and animal chow (Snif Voer, Soest, The Netherlands).

Biodistribution studies and MicroPET/CT Imaging

Mice with subcutaneous SK-RC-52 xenografts (4 groups, 5 mice/group) or with subcutaneous FaDu xenografts (4 groups, 5 mice/group) were intravenously injected with ^{68}Ga-DOTA-E-[c(RGDfK)]$_2$, ^{68}Ga-TRAP-(RGD)$_3$, ^{68}Ga-FSC-(RGD)$_3$, or ^{68}Ga-THP-(RGD)$_3$ (0.5 nmol, 15 MBq in 0.3 ml) in the tail vein of awake mice. Mice were warmed with a heat lamp for several minutes prior to injection. To study the non-$\alpha_v\beta_3$ integrin-mediated localization of the four ^{68}Ga-labelled RGD peptides, separate groups of mice (8 groups, 3 mice/group) were co-injected with a 50 nmol (86 μg) excess of unlabelled DOTA-E-[c(RGDfK)]$_2$.

All mice were euthanized by CO_2/O_2-asphyxiation one hour after injection and tissue samples were dissected and weighed. Additionally, salivary glands of mice bearing FaDu xenografts were dissected and weighed. The uptake of the radiolabelled RGD peptides was calculated as the fraction of injected dose, as determined by gamma counter whilst simultaneously measuring 1% standards, per gram of tissue (%ID/g).

MicroPET/CT scans were obtained directly after euthanasia (2-3 mice/group). Mice were positioned in supine position in the MicroPET/CT scanner (Inveon, Siemens Preclinical Solutions, Knoxville, TN, USA), with an intrinsic spatial resolution of 1.5 mm. Mice were consecutively scanned for 20, 30, or 40 minutes to acquire PET data. For anatomical localisation a CT scan was acquired directly after PET, with a spatial resolution of 113 μm (80 kV, 500 μA, exposure time 300 ms).

PET data were reconstructed using Inveon Acquisition Workplace software version 2.04 (Siemens Preclinical Solutions, Knoxville, TN, USA), using an ordered subset expectation maximisation 3-D (OSEM3D), with a matrix of 256×256×161, pixel size of 0.40×0.40×0.796 mm^3, 16 OSEM3D subsets and 2 iterations. Post reconstruction filtering was performed using 3D Gaussian filter kernel with full width half maximum of 1.5 mm. CT data were reconstructed using a modified Feldkamp algorithm with the same reconstruction software. The resulting matrix was 768x786 pixels with 512 transverse slices (voxel size of 110.5×110.5×110.5 μm^3). PET and CT images were fused for anatomical reference using automatic rigid registration software available at the workstation. Before visualization of tracer accumulation within tumour tissue and other organs, the registration was visually checked.

Statistical analysis

The IC$_{50}$-values of the four ^{68}Ga-labelled RGD peptides were calculated using a non-linear regression model in GraphPad Prism version 5.03 (GraphPad Software, San Diego, CA, USA). Data from the biodistribution studies were expressed as mean percentage injected dose per gram (%ID/g) ± standard deviation (SD). Differences in tracer uptake among the four ^{68}Ga-labelled RGD peptides in the tumour, blood, and salivary glands (as an example of relevant normal tissue) were determined in SPSS Statistics Version 22.0.0.1 (IBM, Armonk,

New York) using a one-way ANOVA followed by post hoc test Bonferroni correction to correct for multiple comparisons. The level of significance was set to $p<0.05$.

Results

Radiolabelling

Labelling efficiency of all four compounds was >95% labelling efficiency as determined with ITLC and HPLC. Mean specific activities after radiolabelling were 49.1 MBq/nmol (^{68}Ga-DOTA-E-[c(RGDfK)]$_2$), 42.3 MBq/nmol (^{68}Ga-TRAP-(RGD)$_3$), 55.2 MBq/nmol (^{68}Ga-FSC-(RGD)$_3$), and 42.6 MBq/nmol (^{68}Ga-THP-(RGD)$_3$). Retention times in the HPLC elution profiles ranged from 11.9 to 14.9 minutes.

Competitive binding assay (IC_{50})

The IC_{50}-values of DOTA-E-[c(RGDfK)]$_2$, TRAP-(RGD)$_3$, FSC-(RGD)$_3$, and THP-(RGD)$_3$ for $\alpha_v\beta_3$ integrin were determined in a competitive binding assay. Binding to $\alpha_v\beta_3$ integrin of ^{111}In-labelled DOTA-E-[c(RGDfK)]$_2$ was determined in the presence of increasing concentrations of unlabelled peptide (Supplementary figure 1). The IC_{50}-value of dimeric DOTA-E-[c(RGDfK)]$_2$ (3.8 ± 0.7 nM) was significantly lower than that of the trimeric compounds TRAP-(RGD)$_3$ (IC_{50} = 10.0 ± 1.8 nM, p=0.005), FSC-(RGD)$_3$, (IC_{50} = 9.0 ± 1.6 nM, p=0.006), and THP-(RGD)$_3$ (IC_{50} = 11.4 ± 1.9 nM, p=0.003). There was no statistically significant difference among the IC_{50} of the trimeric compounds (p=0.7).

Biodistribution studies

The biodistribution profiles one hour after injection of ^{68}Ga-labelled DOTA-E-[c(RGDfK)]$_2$, TRAP-(RGD)$_3$, FSC-(RGD)$_3$, and THP-(RGD)$_3$ in mice with subcutaneous SK-RC-52 and FaDu tumours are summarized in figure 2. The experiments were carried out in two sessions within four consecutive days.

In the SK-RC-52 model, mean tumour uptake of ^{68}Ga-FSC-(RGD)$_3$ (12.5±2.5 %ID/g) was significantly higher compared to that of ^{68}Ga-DOTA-E-[c(RGDfK)]$_2$ (5.3±1.9 %ID/g, p<0.0005), ^{68}Ga-TRAP-(RGD)$_3$ (4.4±0.8 %ID/g, p<0.0005), and ^{68}Ga-THP-(RGD)$_3$ (5.3±0.6 %ID/g, p<0.0005), whereas in the FaDu model, tracer uptake of ^{68}Ga-FSC-(RGD)$_3$ (1.9±0.3 %ID/g) was only significantly higher compared to ^{68}Ga-TRAP-(RGD)$_3$ (1.0±0.2 %ID/g, p=0.026) and was not significantly different from ^{68}Ga-DOTA-E-[c(RGDfK)]$_2$ (1.6±0.5 %ID/g, p=1.0) and ^{68}Ga-THP-(RGD)$_3$ (2.2±0.7 %ID/g, p=1.0). The difference in tumour uptake between ^{68}Ga-TRAP-(RGD)$_3$ and ^{68}Ga-THP-(RGD)$_3$ was also significantly different (p=0.002) in the FaDu xenograft tumour model.

Co-injection of an excess of unlabelled DOTA-E-[c(RGDfK)]$_2$ with radiolabelled RGD peptides resulted in significantly lower tracer uptake in both the SK-RC-52 and FaDu tumours, demonstrating the receptor-specific uptake of each of the four radiolabelled RGD peptides (Supplementary figure 2 and 3). The tumour-to-blood ratio (TBR) of ^{68}Ga-DOTA-E-[c(RGDfK)]$_2$, ^{68}Ga-TRAP-(RGD)$_3$, ^{68}Ga-FSC-(RGD)$_3$, and ^{68}Ga-THP-(RGD)$_3$ in the SK-RC-52 model were 24.4±16.0, 38.5±3.8, 30.7±8.1, and 13.5±1.5 respectively, which are markedly higher than the TBR of in the FaDu model (5.9±2.9, 5.8±0.9, 3.5±0.6, and

6.8±2.8, respectively). In the SK-RC-52 tumour model, TBR between ^{68}Ga-TRAP-(RGD)$_3$ and ^{68}Ga-THP-(RGD)$_3$ was significantly different (p=0.012). No statistically significant differences among the TBR of the other RGD peptides were observed (p>0.05). Whereas individual differences between the four RGD tracers in SK-RC-52 tumour-to-tissue ratios were observed, comparable FaDu tumour-to-tissue ratios between the four tracers were found (table 1). As an example of a relevant normal tissue, tracer uptake in salivary glands showed statistically significant differences between ^{68}Ga-DOTA-E-[c(RGDfK)]$_2$ (1.2 ± 0.3 %ID/g), ^{68}Ga-TRAP-(RGD)$_3$ (0.7 ± 0.1 %ID/g), ^{68}Ga-FSC-(RGD)$_3$ (2.2 ± 0.3 %ID/g), and ^{68}Ga-THP-(RGD)$_3$ (1.6 ± 0.2 %ID/g) in the FaDu model (figure 3).

MicroPET/CT Images

The microPET/CT images acquired one hour post injection were in line with the biodistribution data. MicroPET/CT images clearly visualized SK-RC-52 tumours, but also showed high uptake in kidneys and intestines (figure 4). Despite the high uptake in normal tissues, uptake of all four tracers was visible in the FaDu tumours, with signal intensities in line with the biodistribution studies (supplementary figure 4).

Discussion

This study systematically compared the *in vivo* targeting characteristics of four ^{68}Ga-labelled multimeric RGD peptides: one dimeric peptide (^{68}Ga-DOTA-E-[c(RGDfK)]$_2$) and three trimeric peptides (^{68}Ga-TRAP-(RGD)$_3$, ^{68}Ga-FSC-(RGD)$_3$, and ^{68}Ga-THP-(RGD)$_3$). We demonstrated receptor-specific uptake of all tracers and showed that $\alpha_v\beta_3$ integrin expression could be imaged by the four RGD peptides not only in an $\alpha_v\beta_3$ integrin-positive tumour model (figure 4), but also in a tumour xenograft model in which $\alpha_v\beta_3$ was only expressed on the tumour vasculature (FaDu) (supplementary figure 4), providing the potential for imaging of low-level integrin expression.

So far, different strategies have been considered to develop RGD-based peptides with optimal imaging characteristics. Previously reported experiments with multimeric RGD peptides including ^{68}Ga-DOTA-E-[c(RGDfK)]$_2$, ^{68}Ga-TRAP-(RGD)$_3$, ^{68}Ga-FSC-(RGD)$_3$, and ^{68}Ga-THP-(RGD)$_3$, showed improved tumour targeting compared to monomeric RGD peptides [8, 14, 16, 17]. In this head-to-head comparison differences in absolute tumour uptake amongst multimeric compounds were observed, with highest tumour uptake for ^{68}Ga-FSC-(RGD)$_3$ in SK-RC-52 tumours and ^{68}Ga-THP-(RGD)$_3$ in FaDu tumours. However, our study also indicated that enhanced tumour uptake of ^{68}Ga-FSC-(RGD)$_3$ and ^{68}Ga-THP-(RGD)$_3$ did not result in improved imaging quality in terms of enhanced tumour-to-normal tissue ratios. Concomitant tracer accumulation in non-target organs, like spleen, kidneys, liver, and duodenum was shown to be $\alpha_v\beta_3$ integrin receptor-mediated (supplementary figure 2), presumably due to $\alpha_v\beta_3$ integrin expression on endothelial cells in these organs [18–20]. These findings are in line with previously published data [8, 19].

Whereas *in vivo* studies with RGD peptides mainly focus on high affinities for $\alpha_v\beta_3$ integrin, fast blood clearance, and *in vivo* stability, successful clinical translation is essentially dependent on high contrast images with low uptake in non-target organs. Quantification of tracer uptake in neovasculature may suffer from increased $\alpha_v\beta_3$ integrin-

mediated uptake in both tumour and non-tumour tissues. Furthermore, adequate interpretation of PET images may be hampered by uptake in background tissues. For example, in patients with head and neck cancer, imaging angiogenesis in tumour lesions could be interfered by uptake in the salivary glands (figure 3). Enhanced tracer accumulation of ^{68}Ga-FSC-$(RGD)_3$ and ^{68}Ga-THP-$(RGD)_3$ in salivary glands was observed, with both tracers showing two-fold higher uptake values as compared to ^{68}Ga-DOTA-E-$[c(RGDfK)]_2$ and ^{68}Ga-TRAP-$(RGD)_3$. Therefore, for selection of the best RGD-based tracer to image $\alpha_v\beta_3$ integrin expressing tumours, tracer uptake in background tissues should be considered. For example, in their study in patients with squamous cell carcinoma of the head and neck, Beer et al. showed that PET/CT images could be interpreted adequately and tumour uptake in the oral cavity could be accurately determined quantitatively using ^{18}F-Galacto-RGD, despite the uptake of the tracer in the salivary glands [21].

In the current study, the *in vivo* tracer behaviour was shown to be different in the two human xenograft models used: a significantly higher tumour accumulation in mice with SK-RC-52 tumours was found for ^{68}Ga-FSC-$(RGD)_3$, whereas in the FaDu model only significantly lower uptake for ^{68}Ga-TRAP-$(RGD)_3$ was observed. The exact mechanism leading to these differences is unknown. It has been hypothesized that the enhanced tumour uptake of multimeric RGD tracers is due to simultaneous binding of more than one RGD unit to $\alpha_v\beta_3$ integrins. However, this is unlikely due to limited spacer length between the RGD units [22, 23]. Hypothetically, the differential $\alpha_v\beta_3$ integrin expression levels in the two models may explain the variation tumour uptake. At the higher $\alpha_v\beta_3$ expression levels in the SK-RC-52 model, affinity enhancement due to statistical rebinding of multimeric RGD tracers might play a more important role [24]. In addition, their pharmacokinetic behaviour may be influenced by the structural arrangement of the conjugated RGD peptides (e.g. distance between the RGD units) and the rigidity of its chelator. Nevertheless, the precise effect of the structure of RGD peptide conjugates on its binding behaviour to $\alpha_v\beta_3$ integrins in various tumour models remains to be elucidated.

Molecular imaging of $\alpha_v\beta_3$ integrin expression with radiolabelled RGD peptides has been studied in several clinical applications. RGD PET/CT has allowed imaging in tumours and their metastases and has provided supporting diagnostic information on tumour angiogenesis, in addition to ^{18}F-FDG PET/CT imaging [25–28]. Radiolabelled RGD analogues have also been studied as tools to monitor therapy response, both preclinically [5] and clinically [28–30]. With the addition of ^{90}Y- and ^{177}Lu, the RGD peptides might even be considered for therapeutic applications [31, 32], although the specific uptake in various normal tissues might limit the activity dose that can be safely administered.

Conclusions

In this study differences in the in vivo targeting characteristics of ^{68}Ga-DOTA-E-$[c(RGDfK)]_2$, ^{68}Ga-TRAP-$(RGD)_3$, ^{68}Ga-FSC-$(RGD)_3$, and ^{68}Ga-THP-$(RGD)_3$ were found. The highest tumour uptake was found for ^{68}Ga-FSC-$(RGD)_3$ and ^{68}Ga-THP-$(RGD)_3$ in the SK-RC-52 and FaDu model, respectively. By considering chemical structure, binding affinity, and tracer uptake in tumour tissue as well as (surrounding) normal tissue, the most

optimal radiopharmaceutical can be selected for specific diagnostic or therapeutic applications with radiolabelled RGD peptides.

Supplementary Material

Refer to Web version on PubMed Central for supplementary material.

Acknowledgments

The authors would like to thank Iris Lamers-Elemans, Kitty Lemmens-Hermans, Bianca Lemmers-van de Weem, and Maikel School of the animal facility for technical assistance during the experiments.

References

1. Brakebusch C, et al. Integrins in invasive growth. J Clin Invest. 2002; 109(8):999–1006. [PubMed: 11956235]
2. Hood JD, Cheresh DA. Role of integrins in cell invasion and migration. Nat Rev Cancer. 2002; 2(2): 91–100. [PubMed: 12635172]
3. Katsamakas S, et al. RGD-mediated delivery of small-molecule drugs. Future Med Chem. 2017; 9(6):579–604. [PubMed: 28394627]
4. Dal Corso A, et al. alphavbeta3 Integrin-Targeted Peptide/Peptidomimetic-Drug Conjugates: In-Depth Analysis of the Linker Technology. Curr Top Med Chem. 2016; 16(3):314–29. [PubMed: 26126915]
5. Terry SY, et al. Can 111In-RGD2 monitor response to therapy in head and neck tumor xenografts? J Nucl Med. 2014; 55(11):1849–55. [PubMed: 25349221]
6. Haubner R, Maschauer S, Prante O. PET radiopharmaceuticals for imaging integrin expression: tracers in clinical studies and recent developments. Biomed Res Int. 2014; 2014:871609. [PubMed: 25013808]
7. Dijkgraaf I, et al. Improved targeting of the alpha(v)beta (3) integrin by multimerisation of RGD peptides. Eur J Nucl Med Mol Imaging. 2007; 34(2):267–73. [PubMed: 16909226]
8. Dijkgraaf I, et al. PET imaging of alphavbeta(3) integrin expression in tumours with (6)(8)Ga-labelled mono-, di- and tetrameric RGD peptides. Eur J Nucl Med Mol Imaging. 2011; 38(1):128–37. [PubMed: 20857099]
9. Poethko T, et al. Improved tumor uptake, tumor retention and tumor/background ratios of pegylated RGD-multimers. Journal of Nuclear Medicine. 2003; 44(5):46p–46p.
10. Thumshirn G, et al. Multimeric cyclic RGD peptides as potential tools for tumor targeting: solid-phase peptide synthesis and chemoselective oxime ligation. Chemistry. 2003; 9(12):2717–25. [PubMed: 12772286]
11. Kim JH, et al. Whole-body distribution and radiation dosimetry of (68)Ga-NOTA-RGD, a positron emission tomography agent for angiogenesis imaging. Cancer Biother Radiopharm. 2012; 27(1): 65–71. [PubMed: 22149685]
12. Knetsch PA, et al. [68Ga]NODAGA-RGD for imaging alphavbeta3 integrin expression. Eur J Nucl Med Mol Imaging. 2011; 38(7):1303–12. [PubMed: 21487838]
13. Notni J, et al. TRAP, a powerful and versatile framework for gallium-68 radiopharmaceuticals. Chemistry. 2011; 17(52):14718–22. [PubMed: 22147338]
14. Notni J, Pohle K, Wester HJ. Be spoilt for choice with radiolabelled RGD peptides: preclinical evaluation of (6)(8)Ga-TRAP(RGD)(3). Nucl Med Biol. 2013; 40(1):33–41. [PubMed: 22995902]
15. Knetsch PA, et al. [(68)Ga]FSC-(RGD)3 a trimeric RGD peptide for imaging alphavbeta3 integrin expression based on a novel siderophore derived chelating scaffold-synthesis and evaluation. Nucl Med Biol. 2015; 42(2):115–22. [PubMed: 25459110]
16. Zhai C, et al. Comparison of Ga-68-Labeled Fusarinine C-Based Multivalent RGD Conjugates and [Ga]NODAGA-RGD-In Vivo Imaging Studies in Human Xenograft Tumors. Mol Imaging Biol. 2016

17. Imberti C, et al. Enhancing PET Signal at Target Tissue in Vivo: Dendritic and Multimeric Tris(hydroxypyridinone) Conjugates for Molecular Imaging of alphavbeta3 Integrin Expression with Gallium-68. Bioconjug Chem. 2017; 28(2):481–495. [PubMed: 27966893]
18. Terry SY, et al. Imaging integrin alphavbeta3 on blood vessels with 111In-RGD2 in head and neck tumor xenografts. J Nucl Med. 2014; 55(2):281–6. [PubMed: 24408894]
19. Wu Z, et al. microPET of tumor integrin alphavbeta3 expression using 18F-labeled PEGylated tetrameric RGD peptide (18F-FPRGD4). J Nucl Med. 2007; 48(9):1536–44. [PubMed: 17704249]
20. Max R, et al. Immunohistochemical analysis of integrin alpha vbeta3 expression on tumor-associated vessels of human carcinomas. Int J Cancer. 1997; 71(3):320–4. [PubMed: 9139861]
21. Beer AJ, et al. [18F]galacto-RGD positron emission tomography for imaging of alphavbeta3 expression on the neovasculature in patients with squamous cell carcinoma of the head and neck. Clin Cancer Res. 2007; 13(22 Pt 1):6610–6. [PubMed: 18006761]
22. Kiessling LL, Pohl NL. Strength in numbers: non-natural polyvalent carbohydrate derivatives. Chem Biol. 1996; 3(2):71–7. [PubMed: 8807830]
23. Liu S. Radiolabeled cyclic RGD peptides as integrin alpha(v)beta(3)-targeted radiotracers: maximizing binding affinity via bivalency. Bioconjug Chem. 2009; 20(12):2199–213. [PubMed: 19719118]
24. Wu Y, et al. microPET imaging of glioma integrin {alpha}v{beta}3 expression using (64)Cu-labeled tetrameric RGD peptide. J Nucl Med. 2005; 46(10):1707–18. [PubMed: 16204722]
25. Beer AJ, et al. Comparison of integrin alphaVbeta3 expression and glucose metabolism in primary and metastatic lesions in cancer patients: a PET study using 18F-galacto-RGD and 18F-FDG. J Nucl Med. 2008; 49(1):22–9. [PubMed: 18077538]
26. Zheng K, et al. 68Ga-NOTA-PRGD2 PET/CT for Integrin Imaging in Patients with Lung Cancer. J Nucl Med. 2015; 56(12):1823–7. [PubMed: 26429958]
27. Mi B, et al. Pilot Prospective Evaluation of (18)F-Alfatide II for Detection of Skeletal Metastases. Theranostics. 2015; 5(10):1115–21. [PubMed: 26199649]
28. Chen SH, et al. RGD-K5 PET/CT in patients with advanced head and neck cancer treated with concurrent chemoradiotherapy: Results from a pilot study. Eur J Nucl Med Mol Imaging. 2016; 43(9):1621–9. [PubMed: 26922351]
29. Luan X, et al. 18F-alfatide PET/CT may predict short-term outcome of concurrent chemoradiotherapy in patients with advanced non-small cell lung cancer. Eur J Nucl Med Mol Imaging. 2016; 43(13):2336–2342. [PubMed: 27631310]
30. Zhang H, et al. Can an 18F-ALF-NOTA-PRGD2 PET/CT Scan Predict Treatment Sensitivity to Concurrent Chemoradiotherapy in Patients with Newly Diagnosed Glioblastoma? J Nucl Med. 2016; 57(4):524–9. [PubMed: 26514171]
31. Shi J, et al. Potential therapeutic radiotracers: preparation, biodistribution and metabolic characteristics of 177Lu-labeled cyclic RGDfK dimer. Amino Acids. 2010; 39(1):111–20. [PubMed: 19941017]
32. Liu Z, et al. Two (9)(0)Y-labeled multimeric RGD peptides RGD4 and 3PRGD2 for integrin targeted radionuclide therapy. Mol Pharm. 2011; 8(2):591–9. [PubMed: 21247151]

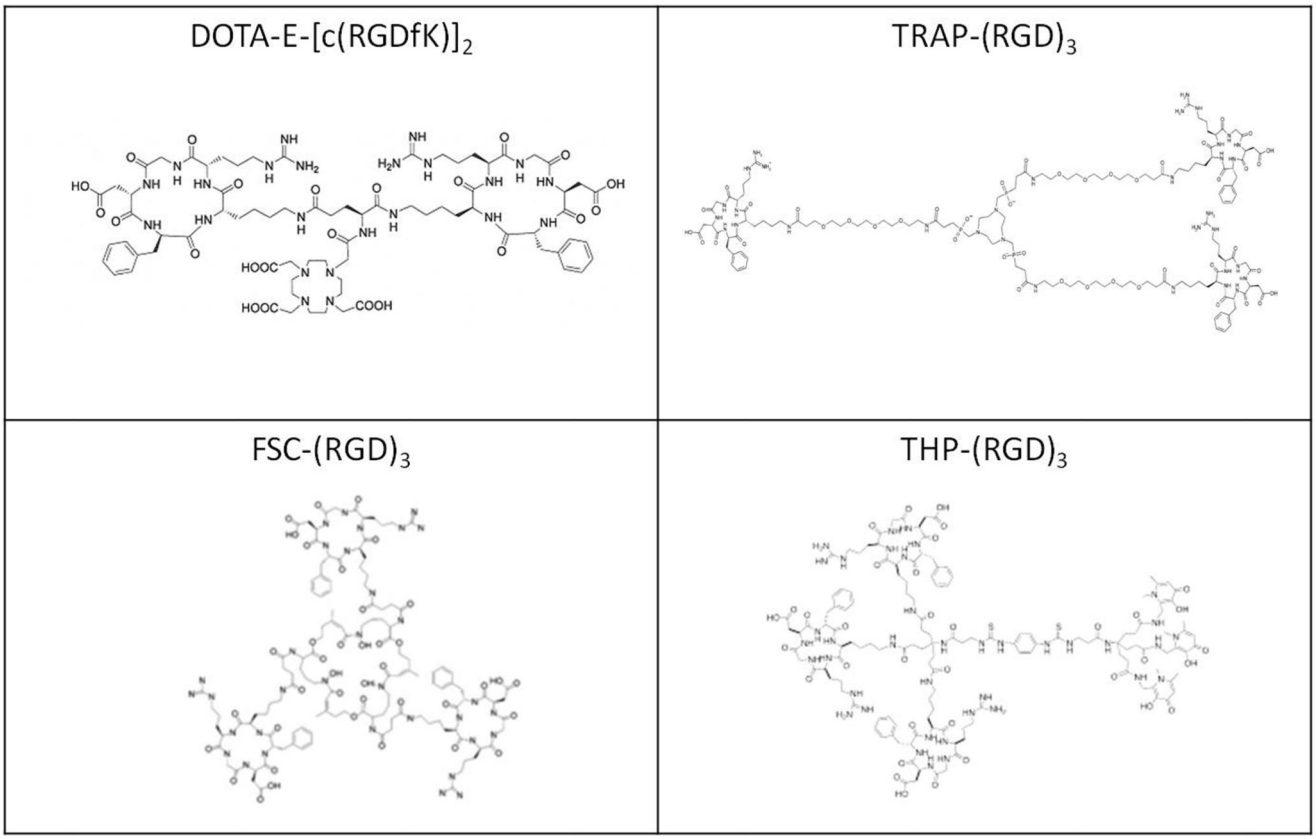

Figure 1.

Structures of unlabelled DOTA-E-[c(RGDfK)]$_2$ (upper left), TRAP-(RGD)$_3$ (upper right), FSC-(RGD)$_3$ (lower left), and ^{68}Ga-THP-(RGD)$_3$ (lower right).

Europe PMC Funders Author Manuscripts

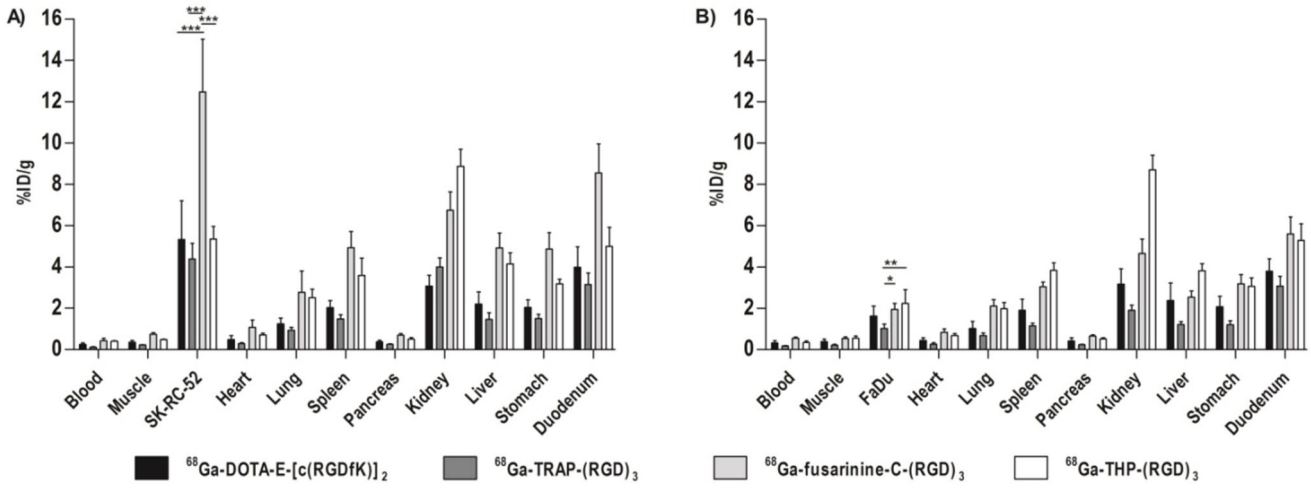

Figure 2.

Biodistribution of ^{68}Ga-labelled RGD peptides in BALB/c nude mice (n=5 per group) with subcutaneous growing SK-RC-52 xenograft tumours (A) or FaDu tumours (B). Tissues and organs were dissected one hour post injection. Values are expressed as mean percentage injected dose per gram ± standard deviation (mean %ID/g ± SD). Peptide dose was 0.5 nmol/mouse. Significant differences in tumour uptake between the different tracers are marked with an asterisk (p<0.05 (*), p<0.01 (**), and p<0.001 (***)).

Europe PMC Funders Author Manuscripts

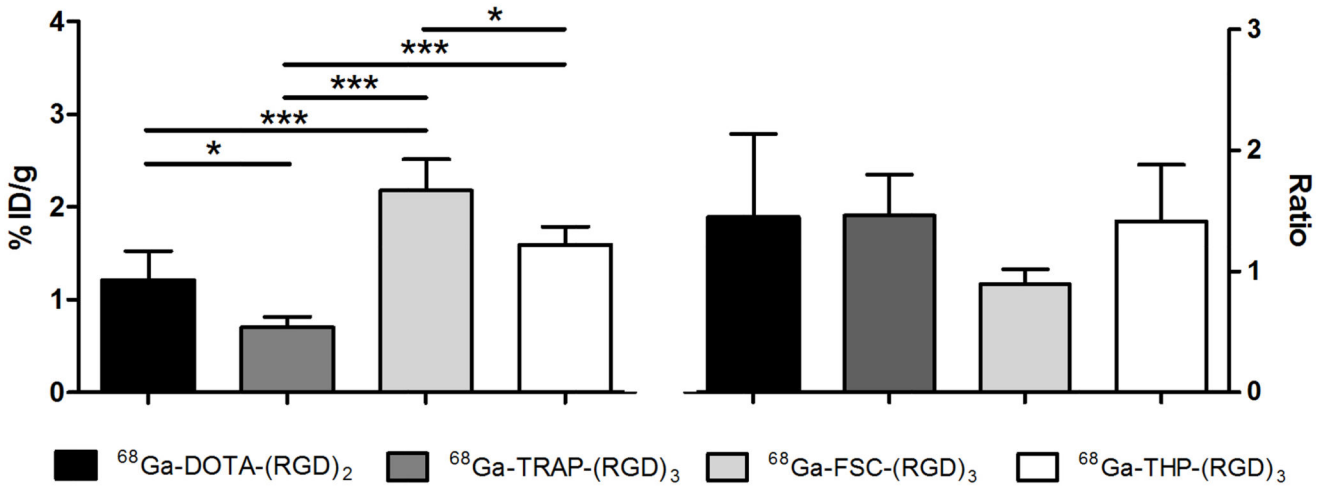

Figure 3.

Tracer uptake (mean %ID/g ± SD) and tumour-to-tissue ratios of the four ^{68}Ga-labelled RGD peptides in salivary glands of BALB/c nude mice with subcutaneously growing FaDu xenograft tumours, one hour post injection. Significant differences in tracer uptake in the salivary glands are marked with an asterisk (p<0.05 (*) and p<0.005 (***)).

Europe PMC Funders Author Manuscripts

Europe PMC Funders Author Manuscripts

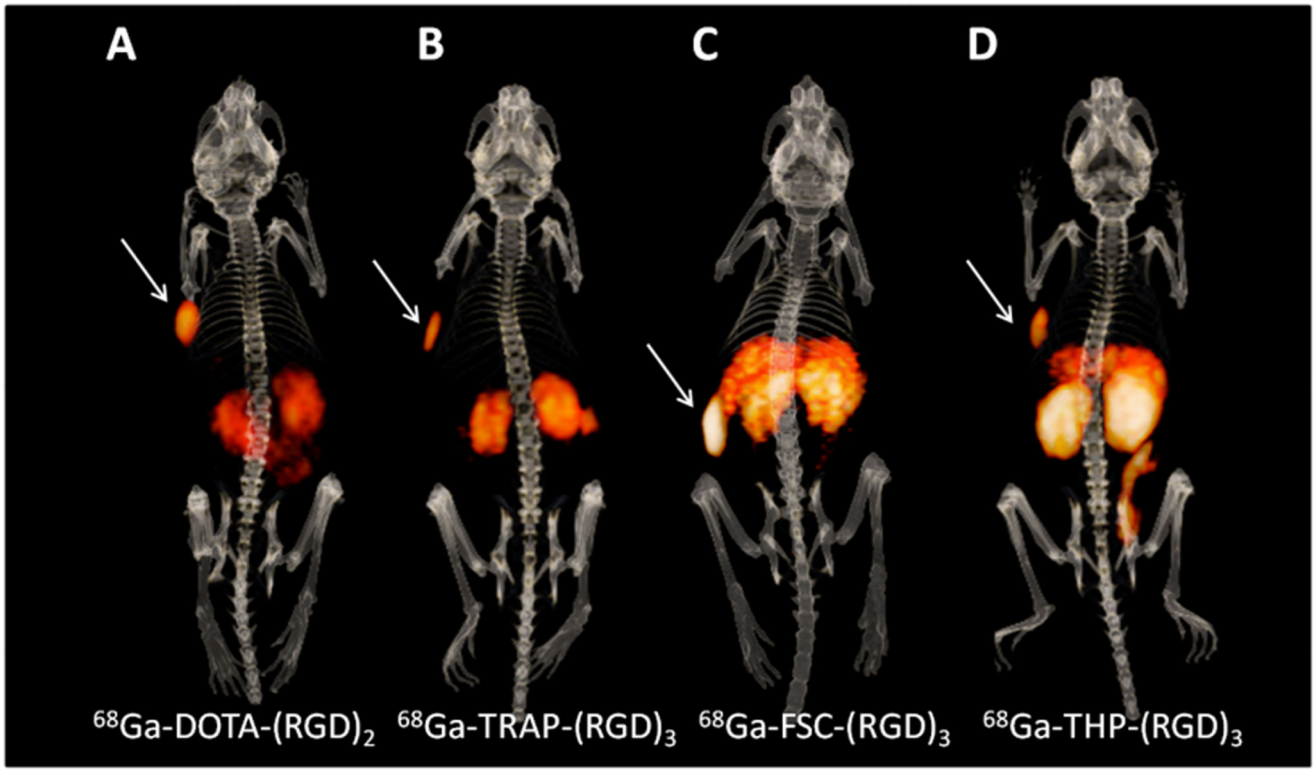

Figure 4.

Typical examples of 3-dimensional microPET/CT images one hour post injection of BALB/c nude mice with subcutaneously bearing SK-RC-52 xenograft tumours in the left flank, indicated with white arrows. Mice were injected with 10-20 MBq, 0.5 nmol ^{68}Ga-DOTA-E-[c(RGDfK)]$_2$ (A), ^{68}Ga-TRAP-(RGD)$_3$ (B), ^{68}Ga-FSC-(RGD)$_3$ (C), or ^{68}Ga-THP-(RGD)$_3$ (D).

Europe PMC Funders Author Manuscripts

Table 1

Tumour-to-normal tissue ratios for ^{68}Ga-DOTA-E-[c(RGDfK)]$_2$, ^{68}Ga-TRAP-(RGD)$_3$, ^{68}Ga-FSC-(RGD)$_3$, and ^{68}Ga-THP-(RGD)$_3$ in BALB/c nude mice bearing SK-RC-52 and FaDu xenografts.

Tumour-to-tissue ratio	^{68}Ga-DOTA-E-[c(RGDfK)]$_2$		^{68}Ga-TRAP-(RGD)$_3$		^{68}Ga-FSC-(RGD)$_3$		^{68}Ga-THP-(RGD)$_3$	
	SK-RC-52	FaDu	SK-RC-52	FaDu	SK-RC-52	FaDu	SK-RC-52	FaDu
Blood	24.4±16.0	5.9±2.9	38.5±3.8	5.8±0.9	30.7±8.1	3.5±0.6	13.5±1.5	6.8±2.8
Muscle	14.7±3.0	4.6±2.3	20.9±3.6	4.8±1.2	17.2±3.2	3.6±0.6	11.3±1.7	4.1±1.2
Heart	12.2±5.4	4.1±2.1	15.3±2.3	4.4±1.4	12.4±3.2	2.4±0.4	7.7±1.7	3.4±1.2
Lung	4.5±2.0	1.9±0.9	4.8±0.9	1.5±0.4	4.8±0.9	0.9±0.1	2.2±0.5	1.2±0.4
Liver	2.5±0.8	0.8±0.5	3.0±0.5	0.8±0.2	2.5±0.2	0.8±0.1	1.3±0.3	0.6±0.2
Spleen	2.7±0.8	0.9±0.4	3.0±0.5	0.9±0.2	2.6±0.5	0.6±0.06	1.6±0.4	0.6±0.2
Pancreas	14.3±4.2	3.8±1.7	17.3±3.7	4.6±1.0	17.9±3.5	3.0±0.4	10.9±2.4	4.5±1.6
Stomach	2.7±1.3	0.7±0.2	3.0±0.7	0.8±0.2	2.6±0.3	0.6±0.1	1.7±0.3	0.7±0.3
Duodenum	1.5±0.9	0.4±0.04	1.4±0.4	0.3±0.07	1.5±0.4	0.4±0.08	0.9±0.3	0.4±0.2
Kidneys	1.7±0.6	0.5±0.2	1.1±0.1	0.5±0.1	1.9±0.3	0.4±0.05	0.6±0.1	0.3±0.08